

New dynamical tide constraints from current and future gravitational wave detections of inspiralling neutron stars

Wynn C. G. Ho*

*Department of Physics and Astronomy, Haverford College,
370 Lancaster Avenue, Haverford, PA, 19041, USA*

Nils Andersson

*Mathematical Sciences and STAG Research Centre,
University of Southampton, Southampton SO17 1BJ, UK*

(Dated: July 21, 2023)

Previous theoretical works using the pre-merger orbital evolution of coalescing neutron stars to constrain properties of dense nuclear matter assume a gravitational wave phase uncertainty of a few radians, or about a half cycle. However, recent studies of the signal from GW170817 and next generation detector sensitivities indicate actual phase uncertainties at least twenty times better. Using these refined estimates, we show that future observations of nearby sources like GW170817 may be able to reveal neutron star properties beyond just radius and tidal deformability, such as the matter composition and/or presence of a superfluid inside neutron stars, via tidal excitation of g-mode oscillations. Data from GW170817 already limits the amount of orbital energy that is transferred to the neutron star to $< 2 \times 10^{47}$ erg and the g-mode tidal coupling to $Q_\alpha < 10^{-3}$ at 50 Hz (5×10^{48} erg and 4×10^{-3} at 200 Hz), and future observations and detectors will greatly improve upon these constraints. In addition, analysis using general parameterization models that have been applied to the so-called p-g instability show that the instability already appears to be restricted to regimes where the mechanism is likely to be inconsequential; in particular, we show that the number of unstable modes is $\ll 100$ at $\lesssim 100$ Hz, and next generation detectors will essentially rule out this mechanism (assuming that the instability remains undetected). Finally, we illustrate that measurements of tidal excitation of r-mode oscillations in nearby rapidly rotating neutron stars are within reach of current detectors and note that even non-detections will limit the inferred inspiralling neutron star spin rate to < 20 Hz, which will be useful when determining other parameters such as neutron star mass and tidal deformability.

I. INTRODUCTION

Measurements of gravitational waves (GWs) from coalescing neutron star (NS) systems provide invaluable insights into the dense matter that comprises the interior of these stars. As is now well-known, the detection of GWs from the inspiral and merger of GW170817 enabled new constraints on the nuclear equation-of-state through determination of the radius and tidal deformability of each NS [1, 2]. With advancements in GW detector sensitivities, it may be possible to obtain measurements from future discoveries that provide constraints which go beyond just bulk NS properties. One example, which is the subject of the current work, is dynamical tidal excitation of NS oscillation modes. Such a process can occur as the orbital frequency increases during the binary inspiral and comes into resonance with the natural oscillation frequencies of the NS. As a result, energy can be transferred between the orbit and the stellar oscillation, which causes the inspiral to occur more rapidly (or more slowly) and creates a phase shift in the GW signal. By measuring the phase shift and GW frequency at which the phase shift occurs, it may then be possible to infer physical properties of the specific oscillation mode, for example, the

particle fractions in the NS or the superfluid state of the star's core.

In this work, we will only be concerned with mode, orbital, and GW frequencies below a few hundred Hz, i.e., well before NS merger, where differences in current GW waveform models are much smaller than the estimated data uncertainties [3]. As such, the strongest coupling between the gravitational tidal potential and an oscillation mode (characterized by $\alpha = nlm$, where n is the number of radial nodes of the mode displacement eigenfunction ξ_α and l and m are indices of the spherical harmonics Y_{lm}) will be through g-modes (see Section IV for r-modes). These g-modes are fluid oscillations whose restoring force is buoyancy caused by, for example, changes in the proton to neutron or muon to electron fraction as a function of density, with the latter being important when neutrons are superfluid [4, 5]. Furthermore, by considering only the leading order tidal quadrupole and primarily non-rotating stars, one only needs to consider the quadrupole modes with $l = 2$. The strength of the tide-mode coupling is determined by the (dimensionless) overlap integral $Q_\alpha = (1/MR^l) \int d^3x \rho \xi_\alpha^* \cdot \nabla(r^l Y_{lm})$, where M and R are stellar mass and radius, respectively, and ρ is mass density [6]. Early works found the largest Q_α ($\sim 10^{-3}$) for low n g-modes [7, 8] and that these values of Q_α produce phase shifts $\Delta\Phi \sim 10^{-3}$ rad [7, 9], which were thought to be too small to be detectable given estimates of GW detector uncertainties at that time (see below).

* wynrho@slac.stanford.edu

A related phenomena which we also examine here is the p-g instability, where instead of tidal resonances with specific oscillation modes during the inspiral, instabilities between coupled p and g-modes supposedly become excited by the tidal potential at GW frequencies f of a few tens of Hz and the orbit loses energy continuously to these modes throughout the remainder of the inspiral [10–13]. Because the p-g instability is not a resonant process and the energy loss occurs over a larger frequency range, a change in phase can gradually build up to large values during the NS inspiral, and hence it was suggested that the instability could strongly alter the GW signal. It was originally estimated that an effective p-g instability amplitude $A_0 \gtrsim 10^{-8}$ would produce phase shifts $\Delta\Phi \gtrsim 1$ rad [12], although subsequent work in [13] found this amplitude to be underestimated by a factor of $\sim (4 - n_0)$ (cf. Section III), where n_0 describes the frequency dependence of the p-g instability and is of order unity.

To be able to measure tidal excitation of g-modes or the p-g instability, the phase uncertainty of detected GWs must be smaller than the phase shift $\Delta\Phi$ (or change in number of orbital cycles $\Delta N = \Delta\Phi/2\pi$) predicted by the theory of these processes. In the works cited above, as well as others, the phase uncertainty was assumed to be either $\Delta\Phi \approx 1\text{--}3$ rad, based on an estimate of a detection with signal-to-noise ratio of 10 and an approximate single detector sensitivity [14, 15], or $\Delta\Phi = \pi$ (or $\Delta N = 0.5$), based on simple matched-filter arguments. However, recent works quantified the level of uncertainty of measured or measurable GWs. Specifically in [16], analysis of the signal from GW170817 using the GW waveform model IMRPhenomPv2_NRTidal [17], which includes effects of static tidal deformabilities, find $\Delta\Phi \sim \pm 0.1$ rad (or $\Delta N \sim \pm 0.03$) at GW frequencies $f < 300$ Hz, inclusive of calibration uncertainties. This uncertainty is shown in Figure 1; note that while $\Delta\Phi$ deviate from zero at 1σ for some frequencies, they are consistent with zero at 2σ , as shown in Figure 12 of [16]. More recently, [3] compares a number of GW waveform models and shows the uncertainty due to waveform differences, and hence the likely best possible uncertainty at the present time, is $\sim \pm 0.02$ rad for A+ and $\pm 10^{-3}$ rad for Cosmic Explorer (CE); we do not consider here the Einstein Telescope (ET), but it is expected to have similar phase uncertainties to CE. Since these phase uncertainties are determined from comparisons between measured/expected GW data and waveform models, they can serve as upper limits on any effects that the waveform models do not take into account but could be present in actual GW data, such as the influence of dynamical tides (see, e.g., [14, 18, 19]).

Given the magnitudes of the phase uncertainty of current detectors and A+ and CE, it is clear that the previously adopted level of phase shift necessary for dynamical tide effects (see, e.g., [5]) is too conservative by at least a factor of 20. Thus future detectors are more likely to detect these effects, which motivates reconsideration and

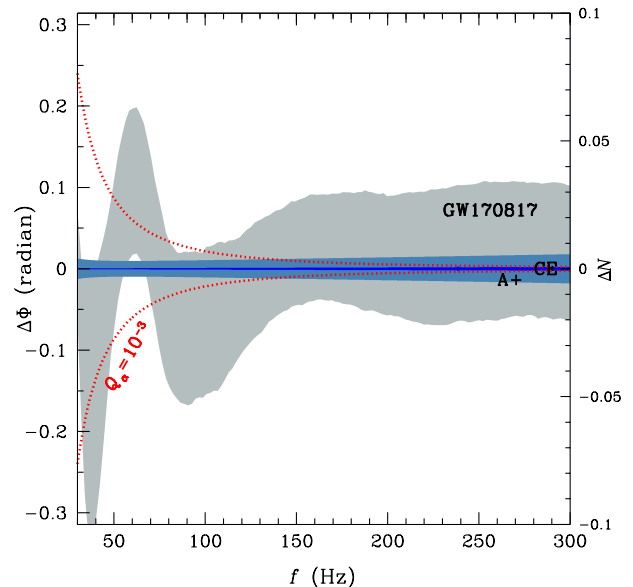


FIG. 1. Phase uncertainty as a function of GW frequency f . Shaded regions indicate $\pm 1\sigma$ deviation of $\Delta\Phi$ from a GW170817 waveform ([16]; see text) and from a model waveform weighted by the sensitivity of A+ and Cosmic Explorer (CE) [3] at a distance of 40 Mpc. Dotted lines indicate $\pm \Delta\Phi$ assuming (dimensionless) overlap integral $Q_\alpha = 10^{-3}$ and NS radius $R = 12$ km [see eq. (7)].

points to work that is needed to maximize the science that can be extracted from future observations. With this aim in mind, we revisit our previous analysis [5] and re-evaluate the detectability of g-modes (in Section II) and the p-g instability (in Section III) in inspiralling NSs (see Section IV for comments on r-modes).

II. ORBITAL ENERGY TRANSFER AND G-MODE RESONANCE

We do not repeat here derivations of the relevant equations, since they are contained in many previous works, and simply state the main relations, following closely the Newtonian orbit calculations of [7] (see also [5]). An estimate of the shift in orbital phase $\Delta\Phi$ due to energy transfer ΔE during orbital decay is

$$\begin{aligned} \frac{\Delta\Phi}{2\pi} &\approx -\frac{t_D}{t_{\text{orb}}} \frac{\Delta E}{|E_{\text{orb}}|} \\ &= -\frac{5c^5}{128\pi} \frac{1}{(GM_1\Omega_{\text{orb}})^{5/3}} \frac{(1+q)^{1/3}}{q} \frac{\Delta E}{|E_{\text{orb}}|} \\ &= -430 M_{1.4}^{-5/3} \left(\frac{1+q}{2q^3}\right)^{1/3} \left(\frac{f}{100 \text{ Hz}}\right)^{-5/3} \frac{\Delta E}{|E_{\text{orb}}|} \quad (1) \end{aligned}$$

where the orbital energy is

$$\begin{aligned} E_{\text{orb}} &= -\frac{GM_1M_2}{2a} \\ &= -1.7 \times 10^{52} \text{ erg } M_{1.4}^{5/3} q \left(\frac{2}{1+q}\right)^{1/3} \left(\frac{f}{100 \text{ Hz}}\right)^{2/3} \quad (2) \end{aligned}$$

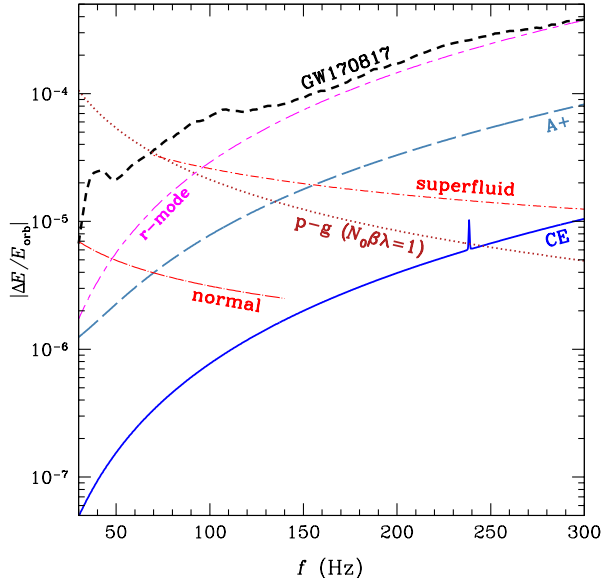


FIG. 2. Relative energy transfer $|\Delta E/E_{\text{orb}}|$ as a function of GW frequency f . Thick lines are upper limits calculated using $\pm\Delta\Phi$ from Fig. 1 and eq. (1) for GW170817 (short-dashed), A+ (long-dashed), and Cosmic Explorer (CE; solid). Long-dashed-dotted and short-dashed-dotted lines are for total energy transferred to normal and superfluid g-modes, respectively (see text for details), while the dotted line is for total energy dissipated by the p-g instability assuming NS radius $R = 12$ km and $N_0\beta\lambda = 1$ [see eq. (8)] and the short-long-dashed line is for energy transferred to the orbit by r-modes and $R = 12$ km [see eq. (12)]. Note that for the r-mode, each particular GW frequency corresponds to a specific NS spin frequency [here we assumed $f = (4/3)f_{\text{spin}}$].

for binary masses M_1 and M_2 , mass ratio $q = M_2/M_1$, orbital separation a , and orbital frequency $\Omega_{\text{orb}} (= \pi f)$. We also note that the chirp mass $\mathcal{M} = (M_1 M_2)^{3/5}/(M_1 + M_2)^{1/5} = M_1[q^3/(1+q)]^{1/5}$. The two timescales are the orbital period $t_{\text{orb}} = 2\pi/\Omega_{\text{orb}}$ and orbital decay timescale

$$t_D \equiv \frac{a}{|\dot{a}|} = \frac{5c^5}{64G^3} \frac{a^4}{M_1 M_2 (M_1 + M_2)} \\ = 8.6 \text{ s } M_{1.4}^{-5/3} \left(\frac{1+q}{2q^3}\right)^{1/3} \left(\frac{f}{100 \text{ Hz}}\right)^{-8/3}. \quad (3)$$

For simplicity, we assume $M_{1.4} = M_1/1.4 M_{\text{Sun}} = 1$ and $q = 1$ throughout the present work.

As noted in the Introduction, the phase uncertainties shown in Figure 1 are derived from comparisons between the measured or expected GW data and waveform models. Since these waveform models do not include dynamical tidal effects such as the resonant excitation of oscillation modes at low frequencies well before merger, $\Delta\Phi$ from Figure 1 illustrates the potential to constrain these unmodeled contributions to actual GW data. In Figure 2, we show inferred upper limits on energy transfer during the inspiral obtained by substituting $\Delta\Phi$ from

Figure 1 into equation (1). Also shown are the calculated total energy transferred to normal and superfluid g-mode oscillations from [20] (for $l = 2$ and summed over $n = 1, 2, \dots, 8$). Note that the (model-dependent) frequencies of the $n = 1$ and $n = 8$ normal g-modes are approximately 140 Hz and 20 Hz, respectively, while the corresponding frequencies for superfluid g-modes are 430 Hz and 70 Hz [20]; superfluid g-modes occur at higher frequencies than normal g-modes of the same n (by about a factor of the square root of proton fraction; [4, 21]).

We see from Figure 2 that the sensitivity of detectors available at the time of GW170817 is insufficient to observe any transfer of energy from the decaying orbit to either NS with a limit of $|\Delta E/E_{\text{orb}}| \approx 10^{-5} - 10^{-4}$ at $f > 30$ Hz. However, it seems possible that the sensitivity of A+ detectors may be able to begin to measure energy transfers to normal and superfluid g-modes in limited frequency ranges. Meanwhile, CE could measure energy transfer to normal and superfluid g-modes throughout the inspiral.

For resonance with a specific $m = 2$ mode, the relation between mode oscillation frequency ω_α , orbital frequency Ω_{orb} , and gravitational wave frequency f is

$$\omega_\alpha = 2\Omega_{\text{orb}} = 2\pi f. \quad (4)$$

For convenience, the mode oscillation frequency can be made dimensionless via

$$\omega_\alpha = \omega_1 \hat{\omega}_\alpha = 2\pi \times 2170 \text{ Hz } M_{1.4}^{1/2} R_{10}^{-3/2} \hat{\omega}_\alpha, \quad (5)$$

where $\omega_1 = (GM_1/R^3)^{1/2}$ and $R_{10} = R/10$ km, such that $\Omega_{\text{orb}} = \omega_1 \hat{\omega}_\alpha/2$ at resonance. Note that we only consider here resonance with one of the NSs in a binary NS system for simplicity. The energy transfer due to resonant mode excitation is calculated by [7] to be

$$\frac{\Delta E}{|E_{\text{orb}}|} = \frac{\pi^2}{128} \left(\frac{c^2 R}{GM_1}\right)^{5/2} \left(\frac{2}{1+q}\right)^{4/3} \frac{Q_\alpha^2}{\hat{\omega}_\alpha^{1/3}} \\ = 11 M_{1.4}^{-7/3} R_{10}^2 \left(\frac{2}{1+q}\right)^{4/3} Q_\alpha^2 \left(\frac{f}{100 \text{ Hz}}\right)^{-1/3} \quad (6)$$

Substituting equation (6) into equation (1) gives

$$\frac{\Delta\Phi}{2\pi} = -\frac{5\pi}{4096} \left(\frac{c^2 R}{GM_1}\right)^5 \frac{2}{q(1+q)} \frac{Q_\alpha^2}{\hat{\omega}_\alpha^2} \\ = -4800 M_{1.4}^{-4} R_{10}^2 \frac{2}{q(1+q)} Q_\alpha^2 \left(\frac{f}{100 \text{ Hz}}\right)^{-2}. \quad (7)$$

This phase shift occurs in a narrow frequency range since the duration of the resonance is short compared to the inspiral duration in the GW detector frequency band (see, e.g., [7, 22, 23]).

Figure 3 shows upper limits on the overlap integral Q_α obtained by substituting $\Delta\Phi$ from Figure 1 into equation (7). To illustrate how these limits compare approximately to theoretical expectations, we plot values of Q_α

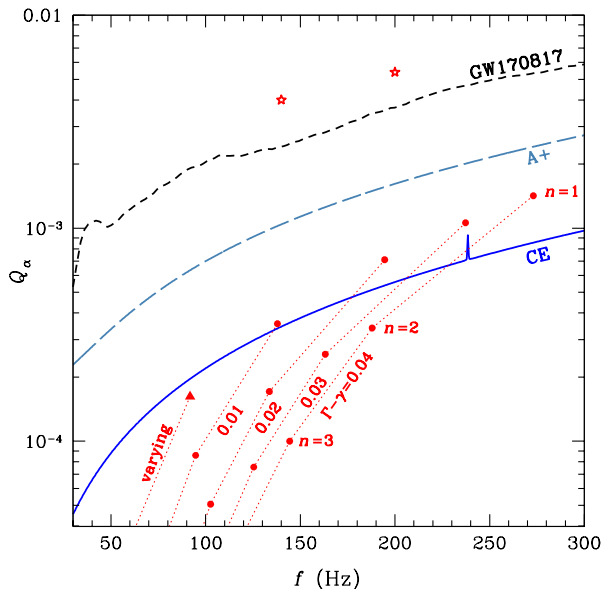


FIG. 3. Dimensionless overlap integral Q_α as a function of GW frequency f . Lines are upper limits calculated using $\pm\Delta\Phi$ from Fig. 1 and eq. (7) with a NS radius $R = 12$ km for GW170817 (short-dashed), A+ (long-dashed), and Cosmic Explorer (CE; solid). Circles are for constant $\Gamma - \gamma$ stratification g-modes, while the triangle is for a varying stratification g-mode (see text); light dotted lines connect Q_α values from g-modes with the same stratification but different radial node n . Stars are for g-modes ($n = 1$) calculated from NS models motivated by the BSk21 and SLy4 equations of state (see Counsell et al., in prep., and [20], respectively), which have strong internal composition gradients.

obtained from NSs constructed in Newtonian gravity using a polytropic ($\gamma = 2$) equation of state and g-modes produced by density stratifications that are parameterized by the factor $(\Gamma - \gamma)$, where Γ is the adiabatic index; results shown are for constant $(\Gamma - \gamma)$ (Counsell et al., in prep.), which reproduce the results of [24], and for a specific case of varying $(\Gamma - \gamma)$ from [24]. [24] find the mode frequency and overlap integral scale as $\omega_\alpha \propto (M/R^3)^{1/2}(\Gamma - \gamma)^{1/2}$ and $Q_\alpha \propto (\Gamma - \gamma)$ for a polytrope with a constant $\gamma = 2$, while [25, 26] find an approximate scaling $\omega_\alpha \propto (M/R^4)^{1/3}(\Gamma - \gamma)^{1/2}$ for NSs constructed using realistic equations of state but still with g-mode stratifications parameterized by $(\Gamma - \gamma)$. Also shown are sample results from Counsell et al. (in prep.) and [20] for Q_α determined using NS models which are motivated by the BSk21 and SLy4 equations of state and have strong varying stratifications. In a sense, these two represent optimistic estimates of Q_α , while those from [26] with $Q_\alpha < 10^{-4}$ are likely to be conservative estimates, and the large range shows the level of uncertainty in current theoretical calculations. Meanwhile, we do not show Q_α for superfluid g-modes in Figure 3 since the ones from [20] would be below the CE curve.

While Figure 2 suggests A+ and CE can constrain

or even measure the total energy transferred to many modes, Figure 3 shows that measuring the coupling to individual modes via the overlap Q_α will be difficult even with CE, although there are evident uncertainties in the theoretical calculations of Q_α , as discussed above. Still, even in the somewhat pessimistic case, we may be able to draw important conclusions about the NS interior. For example, non-detection of individual g-mode coupling with CE could be used to constrain stratification within the NS, e.g., $(\Gamma - \gamma) < 0.02$, or indicate neutrons in the NS core are superfluid. Therefore works such as [20, 25–27] are in the right direction, and more work is needed in using realistic equations of state and stratification to calculate g-modes and their binary tidal interactions. It is also important to keep in mind that Q_α from an extraordinary event, such as an inspiralling NS closer than GW170817, should be within the reach of CE.

III. P-G INSTABILITY

To quantify current and potential future constraints on the p-g instability, we first estimate, from the rate of orbital energy dissipation by the unstable modes \dot{E}_{pg} [see eq. (3) of [12]], that the total energy dissipated is

$$\begin{aligned} \frac{\Delta E}{|E_{\text{orb}}|} &\sim \frac{\dot{E}_{\text{pg}} t_D}{|E_{\text{orb}}|} = 10^{-8} \left(\frac{2}{1+q} \right)^{2/3} \left(\frac{2\pi f}{\omega_1} \right)^{4/3} \omega_1 t_D N_0 \beta \lambda \\ &= 1.9 \times 10^{-5} M_{1.4}^{-11/6} R_{10}^{1/2} \frac{1}{q} \left(\frac{2}{1+q} \right)^{1/3} \\ &\quad \times \left(\frac{f}{100 \text{ Hz}} \right)^{-4/3} N_0 \beta \lambda, \end{aligned} \quad (8)$$

where N_0 is the number of independently unstable modes, β (≤ 1) indicates how close the energy at which unstable modes saturate is to a maximum given by the wave breaking energy, and λ ($\sim 0.1 - 1$) is a slowly varying function of binary separation [11]. Figure 2 plots equation (8) for $N_0 \beta \lambda = 1$, which yields a limit $\Delta E < 4 \times 10^{47}$ erg at $f < 70$ Hz from GW170817. It is argued in [10–12] that $N_0 \sim 100 - 10^4$, but we see that this is only possible if $\beta \ll 0.1$ and $f \lesssim 70$ Hz using just GW170817. This limit would extend to all frequencies of importance for the p-g instability ($\lesssim 100$ Hz; [12, 13]) by the time detectors reach A+ sensitivity.

Next, we consider two parameterizations to determine the effect of the p-g instability on the phase shift $\Delta\Phi$. The first from [13] is

$$\begin{aligned} \Delta\Phi(f > f_0) &= -\frac{2C_0}{3B^2(3-n_0)(4-n_0)} \left(\frac{f}{f_{\text{ref}}} \right)^{n_0-3} \\ &= -2\pi \times 3.1 \times 10^6 M_{1.4}^{-10/3} q^{-2} \\ &\quad \times \frac{A_0}{(3-n_0)(4-n_0)} \left(\frac{100 \text{ Hz}}{f} \right)^{3-n_0} \end{aligned} \quad (9)$$

where $B = (32/5)(GM\pi f_{\text{ref}}/c^3)^{5/3}$, $C_0 = [2/(1+q)]^{2/3} A_0$, f_{ref} ($= 100$ Hz here) is an arbitrary reference

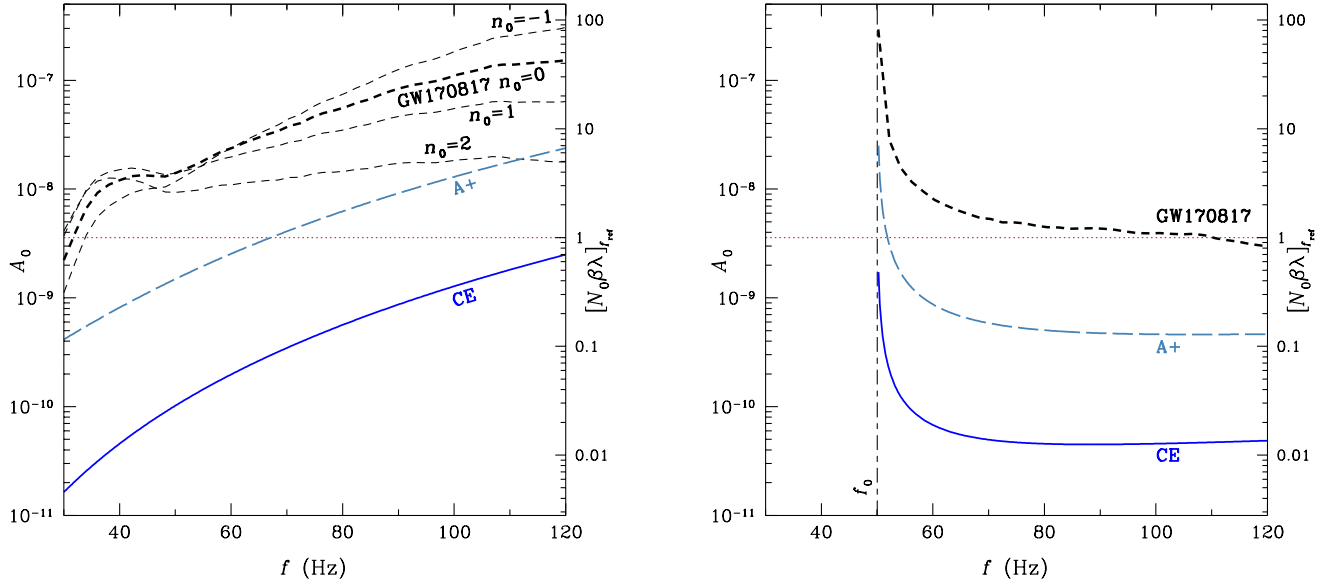


FIG. 4. Amplitude of p-g instability A_0 as a function of GW frequency f . Lines are upper limits calculated using $\pm\Delta\Phi$ from Fig. 1 and the power law model given by eq. (9) (left panel) and the asymptotic model given by eq. (11) (right panel) with frequency power law index $n_0 = 0$ for GW170817 (short-dashed; light lines are for $n_0 = -1, +1, +2$), A+ (long-dashed), and Cosmic Explorer (CE; solid). The vertical line in the right panel indicates the frequency at which mode saturation is assumed to occur, here taken to be $f_0 = 50$ Hz. Parameters of the p-g instability are the number of unstable modes N_0 and mode energy relative to saturation maximum β (≤ 1) and λ ($\sim 0.1 - 1$) is a function of binary separation.

frequency, and n_0 describes the frequency scaling of the orbital energy dissipation rate and is assumed to be in the range $-1 \leq n_0 \leq 3$. Note that the full parameterization of [13] includes dependences on the Heaviside function $\Theta(f - f_0)$, where f_0 (~ 50 Hz; [11, 12]) is the mode saturation frequency, but here we only kept the term that is non-zero at $f > f_0$. In effect, we are ignoring the energy loss before the system reaches saturation, which is reasonable provided the instability grows fast enough. As in the resonance case, we consider the phase contribution due to one NS rather than both. One can relate the amplitude A_0 to $N_0\beta\lambda$ at $f = f_{\text{ref}}$ as discussed in [12], i.e.,

$$\begin{aligned} A_0 &= \left(\frac{2\pi f_{\text{ref}}}{\omega_1}\right)^{1/3} \left(\frac{\omega_g}{\Lambda_g \omega_1}\right)^2 [N_0\beta\lambda]_{f_{\text{ref}}} \\ &= 3.6 \times 10^{-9} \left(\frac{\omega_g}{10^{-4}\Lambda_g \omega_1}\right)^2 [N_0\beta\lambda]_{f_{\text{ref}}}, \end{aligned} \quad (10)$$

where ω_g is the minimum g-mode frequency and $\Lambda_g = l(l+1)$.

The second parameterization is from [12]:

$$\begin{aligned} \Delta\Phi(f > f_0) &= \frac{A_0 F_M}{n_0 - 3} \left(\frac{f_0}{f_{\text{ref}}}\right)^{n_0-3} \left[1 - \left(\frac{f}{f_0}\right)^{n_0-3}\right] \\ &= -2\pi \times 3.1 \times 10^6 M_{1.4}^{-10/3} q^{-2} \\ &\quad \times \frac{A_0}{3 - n_0} \left(\frac{100 \text{ Hz}}{f_0}\right)^{3-n_0} \left[1 - \left(\frac{f}{f_0}\right)^{3-n_0}\right] \quad (11) \end{aligned}$$

where $A_0 F_M = 2C_0/3B^2$. Although [13] points out that this parameterization was calculated incorrectly, it is useful to compare the two since they can be interpreted more generally as models for unknown processes that could affect GW signals, in particular, the former is simply a power law and the latter is asymptotic to a constant phase shift. Specific to the p-g instability, the above two parameterizations of $\Delta\Phi$ differ in amplitude by $\sim (4 - n_0)(f/f_0)^{3-n_0}$ [cf. $(4 - n_0)$ as stated in [13]]. In the more general case, they have very different frequency behavior. Equation (9) implies that $\Delta\Phi \propto (1/f)^{3-n_0}$, so that $A_0 \propto f^{3-n_0}$ for a given $\Delta\Phi$, and hence $\Delta\Phi$ (A_0) decreases (increases) as the frequency increases for $n_0 < 3$. On the other hand, equation (11) states that $\Delta\Phi \propto [1 - (f_0/f)^{3-n_0}]$, so that $\Delta\Phi$ (A_0) increases (decreases) as the frequency increases for $n_0 < 3$ and asymptotes to a constant when $f \gg f_0$.

The left and right panels of Figure 4 show the upper limits on the amplitude A_0 (and $N_0\beta\lambda$) obtained by substituting $\Delta\Phi$ from Figure 1 into equations (9) and (11), respectively. One clearly sees the significantly different amplitudes and frequency behavior described above. Note that the small changes in A_0 at $f \gg f_0$ in the right panel are due to the frequency dependence of the measured/expected $\Delta\Phi$ from Figure 1.

Focusing only on the power law results from the more recent, corrected parameterization of the p-g instability shown in the left panel, we see that the amplitude A_0 is already constrained using GW170817 data to $A_0 < 10^{-7}$ for $n_0 > -1$ at frequencies most relevant to the

instability, i.e., $f \lesssim 100$ Hz. Converting this amplitude A_0 to $N_0\beta\lambda$ using equation (10) and assuming $\beta \sim 1$ and $\lambda \sim 1$, the number of unstable p-g modes is limited to $N_0 \ll 100$ just from GW170817 and could be as low as $N_0 \sim$ a few at $f \lesssim 50$ Hz and/or for $n_0 \gtrsim 2$. The constraint from the amplitude A_0 here is weaker than from energy loss ΔE shown in Figure 2, where the latter gives $N_0\beta\lambda < 1$ at $f < 70$ Hz using GW170817. While there are many uncertainties with the physics of the p-g instability and with our estimates, the p-g instability appears to be much less effective than first suggested. In fact, it may be inconsequential in the evolution of inspiralling NSs. Our analysis can also be interpreted as constraining the amplitude of undetermined mechanisms that are described by the two parameterization models considered above.

A detailed study of GW data from GW170817 specifically searching for effects of the p-g instability was conducted in [13]. The analysis did not provide evidence for effects of the instability but, if assumed to be present, obtained constraints on its parameters f_0 , n_0 , and A_0 . The search for the mode saturation frequency f_0 in the range 10–100 Hz yielded a peak in the posterior distribution at ~ 70 Hz, but such a peak also appeared in simulated data and thus was attributed to noise. The results indicated a slight preference for $n_0 > 2$. An upper limit of $A_0 \approx (3 - 7) \times 10^{-7}$ was obtained, and hence $N_0 \lesssim 200$ at 100 Hz, assuming $\beta = 1$ and $\lambda = 1$. The energy dissipated by the p-g instability was constrained to be $\Delta E < 2 \times 10^{48}$ erg (90% confidence) at $f \leq 70$ Hz. These constraints on A_0 , N_0 , and ΔE from the more comprehensive study are all within a factor of several of our simple estimates.

IV. DISCUSSION

In this work, we showed that recently calculated uncertainties of the phase of GW signals detected from the binary NS inspiral and merger GW170817 and similar uncertainties expected from the future detectors of A+ and CE (and presumably ET) are much smaller than prior work assumed at GW frequencies $f \leq 300$ Hz, where differences in theoretical waveforms are not significant. These smaller $\Delta\Phi$ suggest future detections of nearby merging NSs could begin to measure additional orbital energy loss via mechanisms such as excitation of NS g-mode oscillations. However, the precision in $\Delta\Phi$ may be insufficient to enable measurements of the strength of the coupling between the tidal potential and individual oscillation modes Q_α , unless a very nearby NS inspiral is detected. But it is important to be mindful of the fact that our current values of Q_α are uncertain due to theoretical uncertainties and approximations. In order to make progress, we need accurate relativistic calculations for realistic NS models. At the least, non-detections with CE may provide constraints on particle fractions or superfluid matter inside NSs. We also find that the phase

uncertainty of the signal from GW170817 compared to the phase changes implied by the dissipated energy and amplitude of the p-g instability already limits the number of unstable p-g modes to as low as $N_0 \sim 1$ if the other parameters are at values expected from the model, i.e., $\beta \sim 1$ and $\lambda \approx 0.1 - 1$. Such low values of N_0 indicate the p-g instability is unlikely to produce interesting effects in GW signals from NS mergers, although there are many unknowns here as well.

One avenue that might lead to improved sensitivity to detecting dynamical tidal effects like those studied here is to combine GW signals from multiple inspiralling NS systems. Indeed there are studies of stacking signals to determine how well masses and tidal deformabilities could be measured (see, e.g., [28]). The strategy for the case here would be more complicated as it also involves matter composition, but it is clearly worth exploring. To measure resonances at specific GW frequencies from a stacked signal would require that, e.g., the relation between g-mode frequencies and mass, radius, and stratification are known precisely.

We focused on effects at GW frequencies below 300 Hz because comparisons between current waveforms used to analyze GW data of merging NSs have differences that exceed the measured or expected $\Delta\Phi$ at higher frequencies [3]. This aspect also needs to be addressed. As waveform systematic uncertainties are improved in the coming years, $\Delta\Phi$ at higher frequencies would become limited only by physics not included in the waveforms. Thus these more precise waveforms could be used to constrain the presence of unmodeled physics like those studied here but at higher frequencies, e.g., g-modes in superfluid NSs.

Finally, in Section II, we considered orbital energy loss and GW phase shifts due to resonant excitation of g-mode oscillations during the inspiral. Another potential fluid oscillation that could be resonantly excited gravitomagnetically is a r-mode oscillation [22, 29]. The phase shift from r-mode resonance is estimated by [22] (see also [23]) to be

$$\frac{\Delta\Phi}{2\pi} = 0.006 M_{1.4}^{-10/3} R_{10}^4 \frac{1}{q} \left(\frac{2}{1+q} \right)^{1/3} \left(\frac{f}{100 \text{ Hz}} \right)^{2/3}. \quad (12)$$

Figure 2 shows the result of substituting this into equation (1). We see that the effect of r-mode resonances may be quite significant and could be detectable in the near future. This motivated recent, more detailed calculations, performed in order to estimate how well NS parameters could be extracted from data [18, 19].

There are several important points to note regarding tidal excitation of r-modes. First, the above r-mode phase shift implies energy is transferred to the orbit such that orbital decay is prolonged, although [23] finds there are several related mode resonances that could lead to phase shifts in the opposite direction, depending on the alignment between orbital and NS spin angular momenta. Second, the frequency at which resonance, and thus the phase shift, occurs is proportional to the NS spin rate

f_{spin} , i.e., $f = (4/3)f_{\text{spin}}$ with a slightly larger coefficient after accounting for relativistic effects that depend on M/R [30, 31]. Therefore the NS must be rapidly rotating in order for the resonance to come into effect in the sensitivity band of ground-based detectors. Based on our current understanding and observations of Galactic systems, NSs in binaries that will merge in a Hubble time have spin rates $f_{\text{spin}} < 50$ Hz. For an inspiralling NS-NS system, it is probably unlikely that both NSs would have high enough spin rates for each to have their r-mode resonantly excited during the late stages of inspiral. Most importantly though, detection of a phase delay at a specific frequency would provide independent determinations of M , R , and f_{spin} , which would complement parameters extracted from the conventional inspiral signal and thus could be used to break degeneracies. Even non-detection

could be indicative of a merging NS (or NSs) that has a low spin rate. Thus, while more challenging at lower GW frequencies, detection is possible and an exciting prospect for the era of A+, CE, and ET.

ACKNOWLEDGMENTS

The authors are grateful to Bruce Edelman, Ben Farr, and Jocelyn Read for providing the phase uncertainties from their works (and shown in Figure 1) and to Jocelyn Read for her work and discussions. The authors thank Andrew Counsell for sharing his numerical g-mode results with us. NA gratefully acknowledges support from Science and Technology Facility Council (STFC) via grant number ST/V000551/1.

-
- [1] B. P. Abbott *et al.*, Phys. Rev. Lett. **119**, 161101 (2017).
 [2] B. P. Abbott *et al.*, Phys. Rev. Lett. **121**, 161101 (2018).
 [3] J. Read, Classical and Quantum Gravity **40**, 135002 (2023).
 [4] E. M. Kantor and M. E. Gusakov, Mon. Not. R. Astron. Soc. **442**, L90 (2014).
 [5] N. Andersson and W. C. G. Ho, Phys. Rev. D **97**, 023016 (2018).
 [6] W. H. Press and S. A. Teukolsky, Astrophys. J. **213**, 183 (1977).
 [7] D. Lai, Mon. Not. R. Astron. Soc. **270**, 611 (1994).
 [8] K. D. Kokkotas and G. Schafer, Mon. Not. R. Astron. Soc. **275**, 301 (1995).
 [9] A. Reisenegger and P. Goldreich, Astrophys. J. **426**, 688 (1994).
 [10] N. N. Weinberg, P. Arras, and J. Burkart, Astrophys. J. **769**, 121 (2013).
 [11] N. N. Weinberg, Astrophys. J. **819**, 109 (2016).
 [12] R. Essick, S. Vitale, and N. N. Weinberg, Phys. Rev. D **94**, 103012 (2016).
 [13] B. P. Abbott *et al.*, Phys. Rev. Lett. **122**, 061104 (2019).
 [14] C. Cutler and É. E. Flanagan, Phys. Rev. D **49**, 2658 (1994).
 [15] P. Balachandran and E. E. Flanagan, arXiv e-prints, gr-qc/0701076 (2007).
 [16] B. Edelman, F. J. Rivera-Paleo, J. D. Merritt, B. Farr, Z. Doctor, J. Brink, W. M. Farr, J. Gair, J. S. Key, J. McIver, and A. B. Nielsen, Phys. Rev. D **103**, 042004 (2021).
 [17] T. Dietrich, S. Khan, R. Dudi, S. J. Kapadia, P. Kumar, A. Nagar, F. Ohme, F. Panarale, A. Samajdar, S. Bernuzzi, G. Carullo, W. Del Pozzo, M. Haney, C. Markakis, M. Pürrer, G. Riemenschneider, Y. E. Setyawati, K. W. Tsang, and C. Van Den Broeck, Phys. Rev. D **99**, 024029 (2019).
 [18] S. Ma, H. Yu, and Y. Chen, Phys. Rev. D **103**, 063020 (2021).
 [19] P. K. Gupta, J. Steinhoff, and T. Hinderer, arXiv e-prints, arXiv:2302.11274 (2023).
 [20] H. Yu and N. N. Weinberg, Mon. Not. R. Astron. Soc. **464**, 2622 (2017).
 [21] A. Passamonti, N. Andersson, and W. C. G. Ho, Mon. Not. R. Astron. Soc. **455**, 1489 (2016).
 [22] É. É. Flanagan and É. Racine, Phys. Rev. D **75**, 044001 (2007).
 [23] E. Poisson, Phys. Rev. D **101**, 104028 (2020).
 [24] W. Xu and D. Lai, Phys. Rev. D **96**, 083005 (2017).
 [25] H.-J. Kuan, A. G. Suvorov, and K. D. Kokkotas, Mon. Not. R. Astron. Soc. **506**, 2985 (2021).
 [26] H.-J. Kuan, C. J. Krüger, A. G. Suvorov, and K. D. Kokkotas, Mon. Not. R. Astron. Soc. **513**, 4045 (2022).
 [27] P. B. Rau and I. Wasserman, Mon. Not. R. Astron. Soc. **481**, 4427 (2018).
 [28] M. Agathos, J. Meidam, W. Del Pozzo, T. G. F. Li, M. Tompitak, J. Veitch, S. Vitale, and C. Van Den Broeck, Phys. Rev. D **92**, 023012 (2015).
 [29] N. Andersson and K. D. Kokkotas, International Journal of Modern Physics D **10**, 381 (2001).
 [30] K. H. Lockitch, J. L. Friedman, and N. Andersson, Phys. Rev. D **68**, 124010 (2003).
 [31] A. Idrisy, B. J. Owen, and D. I. Jones, Phys. Rev. D **91**, 024001 (2015).